

Ultra-thin carbon layer for high density magnetic storage devices

C. Casiraghi^a, A.C. Ferrari^{a,*}, J. Robertson^a, R. Ohr^b, M.v. Gradowski^b, D. Schneider^c, H. Hilgers^b

^aEngineering Department, University of Cambridge, Trumpington Street, Cambridge CB2 1PZ, UK

^bIBM STD, Hechtsheimerstrasse 2, D-55131 Mainz, Germany

^cFraunhofer Institute for Material and Beam Technology IWS, Dresden, Germany

Abstract

Storage density is presently doubling every year. This requires the read head to approach closer to the magnetic layer, and ever-thinner layers of carbon. Film thickness below 2 nm and roughness well below 1 nm are needed for the storage of ~ 1 Tb/in². Here we present an analytical and functional characterisation of ultra-thin carbon nitride and pure carbon films produced by magnetron sputtering and filtered high current vacuum arc. The main focus is the effect of nitrogen composition and decreasing film thickness on the relevant mechanical and tribological properties. The carbon bonding has been monitored by using a combination of Raman spectra, taken at two wavelengths (514 and 244 nm). We show that the density, nitrogen content, scratching resistance and Young's modulus of ultra-thin films can all be monitored by the G peak dispersion. Also, the G peak full width at half maximum is a useful parameter in order to investigate the structural evolution of thin films.

© 2003 Elsevier B.V. All rights reserved.

Keywords: Diamond-like carbon; Raman spectroscopy; Coatings; Mechanical properties

1. Introduction

Hard and thin amorphous carbon films are used in the magnetic storage industry to protect read/write head and magnetic media against wear and corrosion. Overcoats currently used are magnetron-sputtered (MS) nitrogenated carbon films (a-C:N) with thickness of 4–5 nm [1–3].

Storage density is presently doubling every year. The ultimate barrier to storage density is the super-paramagnetic limit, where the thermal energy is able to overcome the coercive energy of the magnetic bit. For the longitudinal recording this limit is ~ 100 Gbit/in² [4] whilst the vertical recording should allow storage densities up to ~ 1 Tbit/in² [5,6]. This requires the read head to approach closer to the magnetic layer and ever-thinner layers of carbon 1–2 nm thick [4]. However, a-C:N ceases to provide protection against corrosion and wear in the range of 2–3 nm thickness [7,8]. The low ion energy (approx. 5 eV), involved in the magnetron sputtering, cannot overcome any nucleation barriers. Thus, it is not possible to deposit continuous and ultra-thin film by magnetron sputtering [7,8]. To be protective,

the film should be dense, pin-hole free, smooth and have good mechanical properties.

A new overcoat and a new deposition method are needed for future magnetic storage device. Filtered high current vacuum arc (HCA) is a promising candidate. The main advantages of this process compared to MS are considerably higher degree of ionisation (approx. 90%) and ion energy of 20–40 eV [9]. Pure and nitrogen doped tetrahedral amorphous carbon (ta-C and ta-C:N, respectively) with density up to 3 g/cm³, hardness up to 70 GPa and low roughness (approx. 0.12 nm) can be deposited [9].

The magnetic storage industry needs a quick and non-destructive probe of ultra-thin film. When the thickness drops below 3 nm (approx. 20 atoms thick) it is unlikely that the carbon films can maintain the bulk properties. Raman spectroscopy is a popular and well-established technique in order to study the carbon bonding in amorphous carbon films.

Here, we present a direct comparison of the structural and mechanical properties of MS deposited a-C:N, HCA deposited ta-C and (t)a-C:N thin films. We will show that a combined study of Raman spectra taken at two wavelengths, in the UV and visible regions, allows an assessment of the key parameters (mass density, scratch-

*Corresponding author. Tel.: +44-1223-332659; fax: +44-1223-332662.

E-mail address: acf26@eng.cam.ac.uk (A.C. Ferrari).

ing resistance, Young's modulus, nitrogen content) of any carbon used as a protective overcoat.

2. Experimental

We investigated three sets of samples:

1. a-C:N films deposited with a multiple DC magnetron sputter deposition chambers (Circulus M12) present in the production line of IBM, Mainz [10]. These coatings were deposited on magnetically precoated glass disks and were not lubed or burnished after the deposition process. The deposition temperature was 200 °C in order to achieve magnetic layers with high coercitives. a-C:N films were sputtered from high purity graphite targets in Ar/N₂ gas mixture. By varying the N₂ concentration in the sputter gas, the nitrogen content in the film can be controlled. The N content varies between 0 and 15 at.%. The mass density is approximately 1.8–1.9 g/cm³. The thickness is approximately 5 nm.
2. (t)a-C:N films produced by HCA with a 120° macro-particle filter [11]. These films were deposited on silicon substrate at room temperature. The thickness is approximately 5 nm and the nitrogen content varies between 0 and 15 at.%. The sp³ content ranges from ~10 to ~60%. The mass density is between 2 and 2.9 g/cm³.
3. ta-C films produced by HCA with a 120 macroparticle filter [11]. These films have been deposited on silicon substrate at RT, 120 and 200 °C. The thickness is between 0.9 and 20 nm. The HCA source is a pulsed source, contrary to the FCVA. The films were deposited with ~0.1 pulses/s and frequency of 100 Hz, which corresponds to a deposition rate of ~10 nm/s, to be compared with 0.2–0.8 nm/s of an S bend filtered cathodic vacuum arc [12].

The thickness, the density, the sp³ content and the nitrogen content of all films have been determined by: (i) X-ray reflectivity (XRR) [8,13], assuming a single layer; (ii) X-ray absorption near edge structure (XANES) [14]; (iii) X-ray photoelectron spectroscopy (XPS) [8]. The Young's modulus was measured by laser acoustics waves (LAW) [15] and the scratching resistance by atomic force microscopy (AFM) nano-scratching [16].

Raman measurements were performed with two Renishaw Micro Raman 1000 spectrometers at 514.5 and 244 nm in backscattering geometry. For 514.5 nm excitation and for ultra-thin films the contribution of the Si third order peak at ~1450 cm⁻¹ was carefully removed [17,18]. The spectra were fitted by using a Lorentzian function for D and T peaks and a Breit-Wigner-Fano (BWF) line shape for the G peak.

3. Results

All carbons show common features in their Raman spectra in the 800–2000 cm⁻¹ region, the so called G and D peaks, which lie at approximately 1560 cm⁻¹ and 1360 cm⁻¹, respectively, for visible excitation, and the T peak at approximately 1060 cm⁻¹, which is visible only with UV excitation [19–21]. The G peak is due to the bond stretching of all pairs of sp² atoms in both rings and chains. The D peak is due to the breathing modes of sp² atoms in rings. The T peak is due to the C–C sp³ vibrations [19–21].

In order to analyse the carbon bonding, we study the Raman parameters as a function of the excitation wavelength. A most useful parameter, derived by this study, is the G peak dispersion [20]. The G peak dispersion is defined as the slope of the line connecting the G peak positions, measured at different excitation wavelengths. The G peak dispersion is proportional to the degree of disorder in the film. The G peak of graphite and nano crystalline graphite does not disperse (so that the dispersion is zero), while ta-C shows the highest dispersion (approx. 0.45 cm⁻¹/nm). The G peak dispersion is thus a fingerprint of each different carbon films and allows to solve the non-uniqueness problem usually found for single wavelength excitation, where there can be similar Raman spectra for different samples [19]. This is particularly important for magnetic disk deposition since the films are usually grown at ~200 °C, which can favour the decoupling of the sp² clustering from the sp³ content [19].

Due to the almost linear relation between the G peak wavenumber and the excitation wavelength, we define the G peak dispersion as:

$$G \text{ disp} \left(\frac{\text{cm}^{-1}}{\text{nm}} \right) = \frac{G\text{Pos}(244 \text{ nm}) - G\text{Pos}(514.5 \text{ nm})}{(514.5 - 244) \text{ nm}} \quad (1)$$

For amorphous carbon nitrides we can apply similar concepts as those used for N free carbons [22]. N introduction in high sp³ carbons such as ta-C tends to induce sp² clustering and sp³ to sp² conversion, so we would expect non-uniqueness problems if we would perform single wavelength measurements. However, N introduction in low sp³ samples at high temperature can induce disorder, even if it does not increase the sp³ fraction [22]. We thus expect a different trend of the Raman parameters vs. N content for ta-C:N and a-C:N films, but the same trend as a function of the mechanical properties, such as Young's modulus and scratching resistance.

A multi-wavelength investigation provides another useful parameter, the G peak full width at half maximum (FWHM_G). FWHM_G always decreases as the disorder

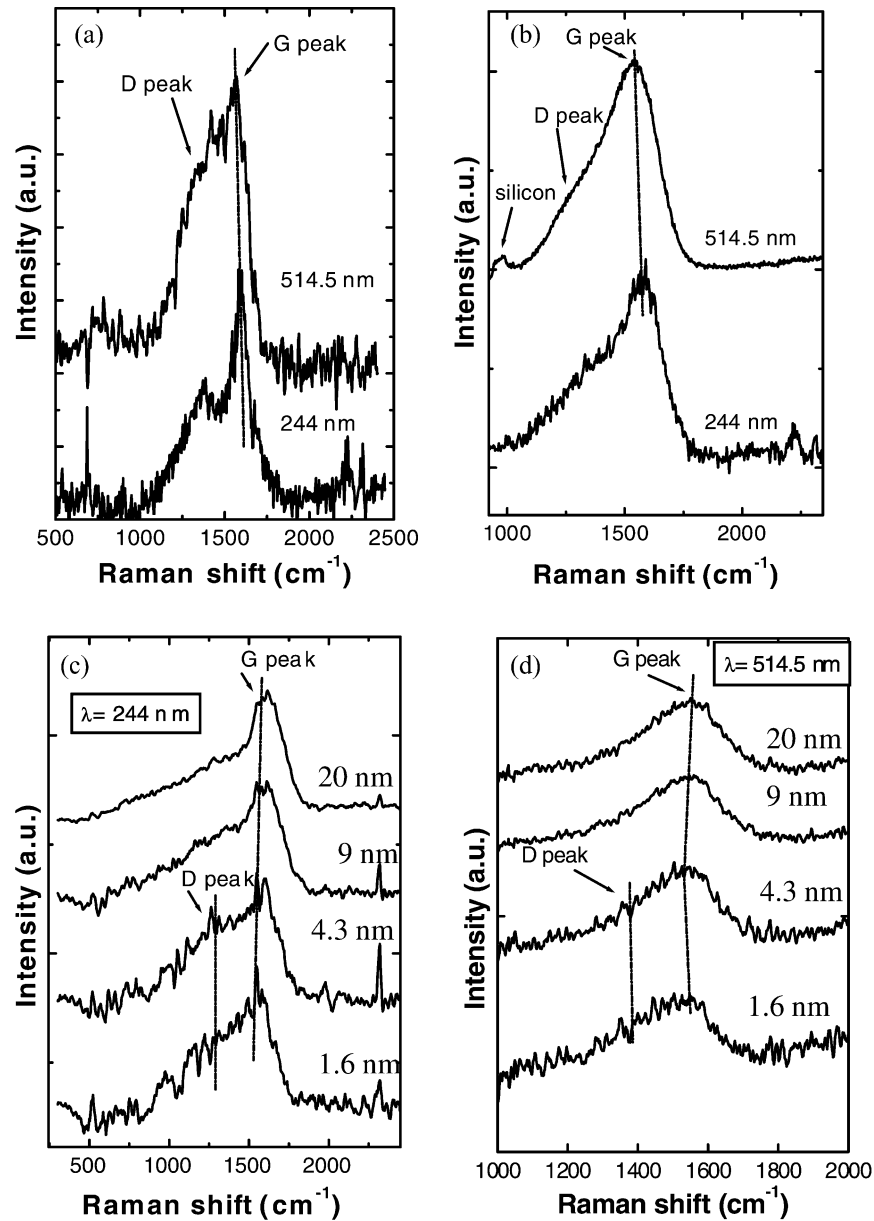


Fig. 1. (a) Raman spectra of MS a-C:N (10% N); (b) Raman spectra of (t)a-C:N (15% N); (c, d) Raman spectra of ta-C of different thickness and excitation wavelength: 244 nm (c) and 514.5 nm (d).

increase, for *every* excitation wavelength and for *every* type of carbon [20,22]. The absolute value of FWHM_G decreases with increasing excitation energy and decreases more for more ordered films [20]. FWHM_G does not present non-uniqueness problems so, in principle, it can monitor the carbon bonding even for a single excitation wavelength. In practise the G peak dispersion, being an averaged parameter over measures at different wavelengths, does have less data scatter than single wavelength FWHM_G . Also, the possibility to check the self-consistency of measurements for at least two different wavelengths, such as 514.5 and 244 nm, gives more reliable data than a single wavelength investigation.

Fig. 1 shows the Raman spectra of MS a-C:N (a), (t)a-C:N (b) and ta-C at 244 nm (c) and 514.5 nm (d). Fig. 2a shows the G peak dispersion of MS a-C:N against N content. The G peak dispersion for a-C:N is always lower than $0.1 \text{ cm}^{-1}/\text{nm}$. The dispersion increases with N content. This confirms that the nitrogen introduction increases the disorder into the sp^2 sites. This is further demonstrated by FWHM_G , which increases with increasing N content, both at 514.5 and 244 nm excitation wavelengths. Fig. 2b shows the G peak dispersion of HCA (t)a-C:N films against N content. Here the G dispersion decreases from 0.24 to $0.1 \text{ cm}^{-1}/\text{nm}$, with increasing N content. Thus, the main

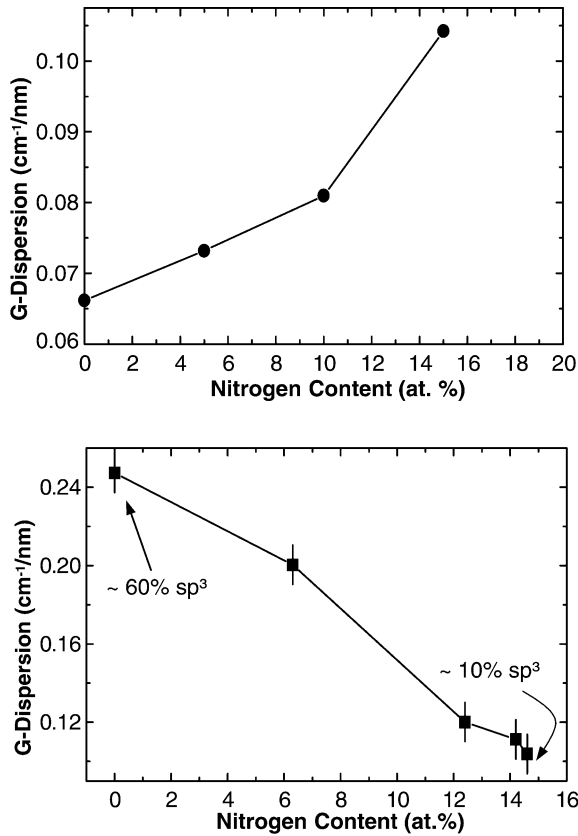


Fig. 2. G peak dispersion as a function of the N content for (a) MS a-C:N and (b) HCA (t)a-C:N.

effect of nitrogen in (t)a-C:N is to induce sp² clustering and reduce the sp³ content [22].

Fig. 3a,b show the G peak dispersion of MS and HCA carbon nitride films against the scratching resistance. The scratching resistance is used by the hard disk industry as a method to assess the mechanical properties of ultra-thin carbon overcoats. It is performed by using an AFM with diamond tips [16]. Using image subtraction, scratches down to a residual depth of 0.1 nm can be evaluated, hence enabling the study of the very beginning of plastic deformation. The scratch resistance is defined by the ratio of the applied loading force and the cross-sectional area of the scratches. The scratching resistance directly relates to the shear modulus and hardness of the carbon overcoats. The elastic constants of amorphous carbons scale with the sp³ fraction and thus with the density [13,23]. The G peak dispersion should thus directly correlate with the scratching resistance. This is clearly shown by Fig. 3a and b, where a linear relation between the G peak dispersion and the scratching resistance of the two sets of films is seen. Note that, comparing Figs. 2 and 3, for MS a-C:N the scratching resistance increases with the N content, whilst for ta-C:N it decreases, as we expect due to the different effect of N in these two sets of films, as previously

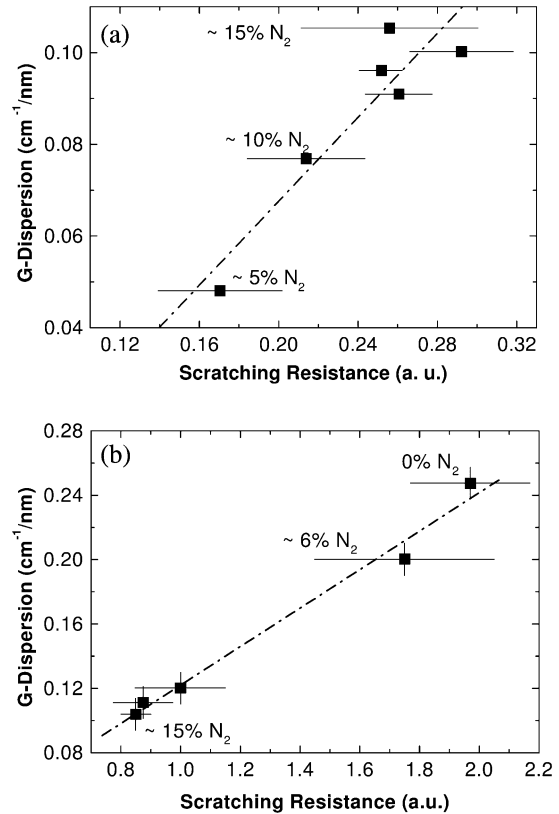


Fig. 3. (a) G peak dispersion of MS a-C:N as a function of the scratching resistance; (b) G peak dispersion of HCA (t)a-C:N as a function of the scratching resistance.

discussed. The expected worsening of the mechanical properties for the HCA (t)a-C:N films with increasing N content is confirmed in Fig. 4, which shows a decrease of Young's modulus and G peak dispersion for films with increasing N content.

Fig. 5a plots the Young's modulus vs. thickness for the N-free HCA ta-C films of set 3. Fig. 5b plots the G peak dispersion for HCA ta-C films against the thick-

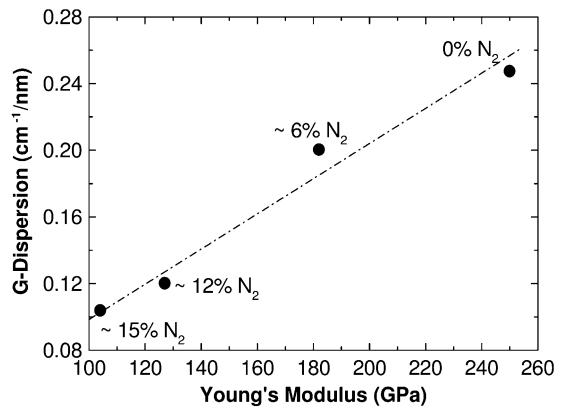


Fig. 4. G peak dispersion of HCA (t)a-C:N as a function of the Young's modulus.

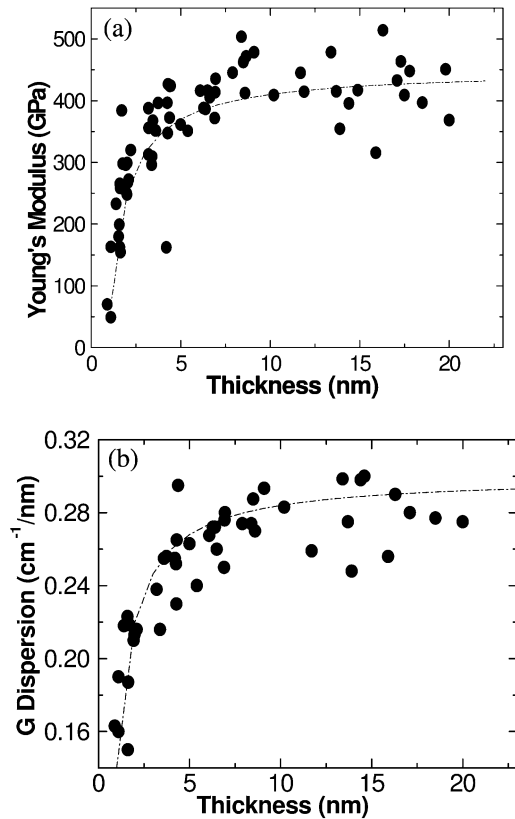


Fig. 5. (a) Young's modulus as a function of thickness for HCA ta-C films; (b) G peak dispersion as a function of thickness for HCA ta-C films. The dotted are a fit to the data with Eq. (2).

ness. The G dispersion strongly decreases below 10-nm film thickness. Also, the FWHM_G decreases from 240 cm^{-1} to 80 cm^{-1} at 244 nm excitation wavelength and from 280 cm^{-1} to 120 cm^{-1} at 633 nm (Fig. 6a and b). This can be understood if we consider the cross sectional structure of ta-C films [13,24,25]. The top-layer is low density and more graphitic. Underneath there is the bulk tetrahedral matrix, which is sp^3 rich. Between the bulk layer and the substrate an interface region is formed. Since the deposition conditions were kept constant during film deposition, the interface and surface layers are roughly independent from the overall thickness [13]. Thus, the thickness reduction results in a reduction in the 'bulk' mainly sp^3 phase. For fixed ion energy, the nature of the surface layer does not change with thickness. When the thickness of the bulk layer becomes similar to the interface and surface layers we expect a strong reduction in the Young's modulus, as observed in Fig. 5a.

The thinnest film for which we measured E is approximately $\sim 1 \text{ nm}$ thick. We can thus assume that no 'bulk' phase is left in this film and thus the combined surface and interface layers Young's modulus (E_{csi}) to be $\sim 50 \text{ GPa}$. We can thus derive a simple expression to describe the evolution of E vs. thickness:

$$E(t) = E_{\text{Bulk}} - (E_{\text{Bulk}} - E_{\text{csi}}) t_{\text{csi}}/t \quad (2)$$

where $E(t)$ is the Young's modulus at a thickness t , E_{Bulk} is the Young's modulus of the bulk phase (which can be approximated with E for $t > 20 \text{ nm}$) and t_{csi} is the total thickness of the surface and interface layers. For the HCA films in Fig. 5a, $t_{\text{csi}} \sim 1 \text{ nm}$, whilst $E_{\text{bulk}} \sim 450 \text{ GPa}$. The dot line in Fig. 5a is a plot of Eq. (2), which yields an excellent agreement, thus confirming our model.

We can then assume Eq. (2) to describe the G Peak dispersion and FWHM_G evolution as a function of thickness, by replacing the E terms in Eq. (2) with the corresponding G peak dispersions and FWHM_G , as shown in Figs. 5b, 6a, 6b.

Finally, Fig. 7 plots the G peak dispersion against the Young's modulus for ta-C films. A linear relation is found, as expected.

4. Conclusion

We investigated different ultra-thin carbon layers used as protective coatings in magnetic storage technology. Resonant Raman spectroscopy has been used successfully to monitor the film structural parameters.

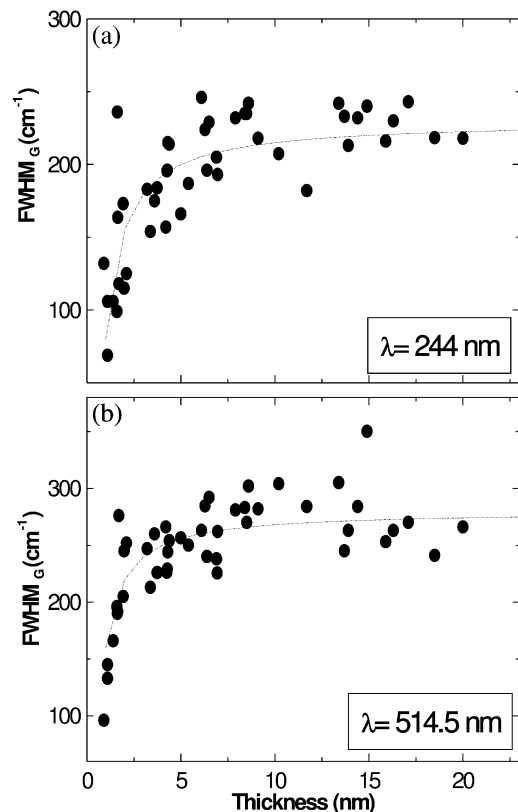


Fig. 6. FWHM_G as a function of thickness for HCA ta-C films of set 3. The FWHM_G are measured at two different excitation wavelengths: (a) 244 nm and (b) 514.5 nm . The dotted lines are a fit to the data with Eq. (2).

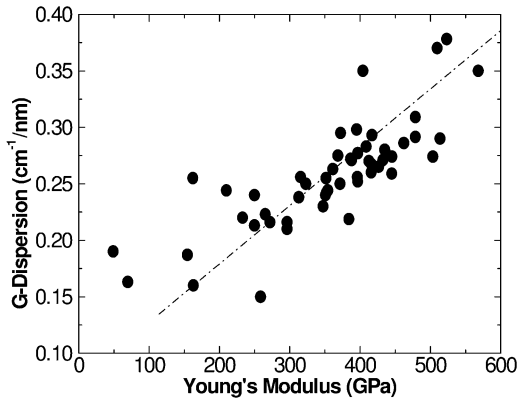


Fig. 7. G peak dispersion of HCA ta-C films of set 3 as a function of the Young's modulus.

The G peak dispersion and FWHM_G are the best way to characterise every type of amorphous carbon film. For any carbon, a decrease of the G peak dispersion and FWHM_G always means ordering and, vice versa, an increase of G peak dispersion and FWHM_G means disordering.

The introduction of nitrogen causes different effects. In MS sputtered a-C:N deposited at high temperature nitrogen increases the disorder, so that the mechanical properties, such as the scratching resistance, slightly increase with the N content. In HCA ta-C the nitrogen induces sp^2 clustering and sp^3 to sp^2 conversion, causing a worsening of the mechanical properties.

When the thickness decreases, the film does not maintain the bulk properties because the thickness reduction mainly shrinks the bulk sp^3 phase, increasing the weight of the softer surface and interface layers.

In any case, a ~ 1 nm thick HCA ta-C film still possesses a Young's modulus of ~ 50 GPa and ~ 2.6 g/cm³ density. Also, it has been shown that the film is continuous, ultra-smooth [26] and corrosion resistant [8]. This satisfies the requirements for the ultimate storage density limit of ~ 1 Tbit/in².

Acknowledgments

The authors thank D. Batchelder, A. Smith and I.R. Mendieta of University of Leeds for UV Raman facilities. Funding from the BMBF project 'Innovative Reaktoren Und In-Situ Analytik Für Nano-Schultzschichten' is acknowledged. CC acknowledges funding from EU

project FAMOUS. ACF acknowledges funding from the Royal Society.

References

- [1] J. Windeln, C. Bram, H.-L. Eckes, D. Hammel, J. Huth, J. Marien, et al., *Appl. Surf. Sci.* 179 (2001) 167.
- [2] E.C. Cutiongco, D. Li, Y.W. Chung, C.S. Bathia, *IEEE Trans. Magn.* 33 (1997) 938.
- [3] A. Leson, H. Hilgers, *Phys. Blatter* 55 (1999) 63.
- [4] P.R. Goglia, J. Berkowitz, J. Hoehn, A. Xidis, L. Stover, *Diamond Relat. Mater.* 10 (2001) 271.
- [5] R.J. Wood, *IEEE Trans. Magn.* 38 (2002) 1711.
- [6] D. Li, M.U. Guruz, C.S. Bhatia, Y. Chung, *Appl. Phys. Lett.* 81 (2002) 1113.
- [7] R.J. Waltman, et al., in: C.S. Bathia (Ed.), *Interface Tribology towards 100 Gbits/in²*, ASME, 1999.
- [8] (a) P. Bernhard, C. Zietzen, R. Ohr, H. Hilgers, G. Schönhense, *Surf. Coat. Technol.* in press
(b) R. Ohr, B. Jacoby, M.v. Gradowski, C. Schug, H. Hilgers, *Surf. Coat. Technol.* 173 (2003) 111.
- [9] T. Witke, P. Siemroth, *IEEE Trans. Plasma Sci.* 27 (1999) 1039.
- [10] M. Neuhaeuser, H. Hilgers, P. Joeris, R. White, J. Windeln, *Diamond Relat. Mater.* 9 (2000) 1500.
- [11] Wienss, G. Persch-Schuy, R. Hartmann, P. Joeris, U. Hartmann, *J. Vac. Sci. Technol. A* 18 (2000) 2023.
- [12] K.B.K. Teo, S.E. Rodil, J.T.H. Tsai, A.C. Ferrari, J. Robertson, W.I. Milne, *J. Appl. Phys.* 89 (2001) 3706.
- [13] A.C. Ferrari, A. Libassi, B.K. Tanner, V. Stolojan, J. Yuan, L.M. Brown, et al., *Phys. Rev. B* 62 (2000) 11089.
- [14] J. Windeln, C. Bram, H.-L. Eckes, D. Hammel, J. Huth, J. Marien, et al., *Appl. Surf. Sci.* 179 (2001) 167.
- [15] D. Schneider, P. Siemroth, T. Schulke, J. Berthold, B. Schultrich, H.-H. Schneider, et al., *Surf. Coat. Technol.* 153 (2002) 252.
- [16] A. Wienss, G. Persch-Schuy, M. Vogelgesang, U. Hartmann, *Appl. Phys. Lett.* 75 (1999) 1077.
- [17] W.P. Acker, B. Yip, Dh. Leach, et al., *J. Appl. Phys.* 64 (1988) 2263.
- [18] C. Casiraghi, A.C. Ferrari, R. Ohr, D.P. Chu, J. Robertson, *Diamond Relat. Mater.*, in press (2004).
- [19] A.C. Ferrari, J. Robertson, *Phys. Rev. B* 61 (2000) 14095.
- [20] A.C. Ferrari, J. Robertson, *Phys. Rev. B* 64 (2001) 075414.
- [21] K.W.K. Gilkes, H.S. Sands, D.N. Batchelder, J. Robertson, W.I. Milne, *Appl. Phys. Lett.* 70 (1997) 1980.
- [22] A.C. Ferrari, S.E. Rodil, J. Robertson, *Phys. Rev. B* 67 (2003) 155306.
- [23] A.C. Ferrari, J. Robertson, M.G. Beghi, C.E. Bottani, R. Ferulano, R. Pastorelli, *Appl. Phys. Lett.* 75 (1999) 1893.
- [24] C.A. Davis, G.A. Amaratunga, K. Knowles, *Phys. Rev. Lett.* 80 (1998) 3280.
- [25] M. Beghi, A.C. Ferrari, K.B.K. Teo, J. Robertson, C.E. Bottani, A. Libassi, et al., *Appl. Phys. Lett.* 81 (2002) 3804.
- [26] C. Casiraghi, A.C. Ferrari, R. Ohr, D.P. Chu, J. Robertson, *Phys. Rev. Lett.* 91 (2003) 226104.